

Cohesive properties and vibrational entropy of 3d transition-metal compounds: MX (NaCl) compounds ($X = \text{C, N, O, S}$), complex carbides, and nitrides

Armando Fernández Guillermet

*Centro Atómico Bariloche, Consejo Nacional de Investigaciones Científicas y Técnicas,
8400 San Carlos de Bariloche, Río Negro, Argentina*

Göran Grimvall

*Department of Theoretical Physics, The Royal Institute of Technology, S-100 44 Stockholm, Sweden
(Received 19 June 1989)*

We let compounds between a 3d transition metal (M) and a nonmetal X ($X = \text{C, N, O, S}$) be characterized by three parameters: the average number of valence electrons per atom (n_e), the average volume per atom (Ω), and the logarithmically averaged atomic mass (M_{eff}). Three quantities with the dimension of energy are then considered: the cohesive energy E_{coh} of the compound, its enthalpy of formation $\Delta^0 H$, and $E_S \equiv M_{\text{eff}}(k_B \Theta_S / \hbar)^2 \Omega^{2/3}$. Θ_S is a Debye temperature, properly defined to give the vibrational entropy at high temperatures. Remarkably accurate empirical relations are found between n_e on one hand and E_{coh} , $\Delta^0 H$, and E_S . For compounds MX of the NaCl crystal structure one can understand the correlation from the electron band structure of (p - d)-bonded systems. We then extend the correlation to carbides and nitrides of more complex structure, for which not much is known about the electron states. The relation between E_S and n_e is of particular importance, since it allows an estimate of cohesive properties and the vibrational entropy in systems where there is no, or uncertain, experimental information. The correlations are applied to e.g., a study of the phase stability of the NaCl structure for large n_e and to the estimation of the standard entropies $^0 S$ and enthalpies of formation $\Delta^0 H$ of various nitrides, carbides, and oxides. We also demonstrate how our method can be coupled with the so-called CALPHAD ("calculation of phase diagrams") work.

I. INTRODUCTION

The relation between the cohesive and thermodynamic properties of solids and their electronic structure is a matter of great theoretical and practical interest. The properties of the static lattice (i.e., essentially properties at $T = 0$ K) may be described by the cohesive energy E_{coh} and the enthalpy of formation $\Delta^0 H$ of the compound. The temperature-dependent part of the Gibbs energy $G(T)$ is usually dominated by the lattice vibrations, which may be described by a properly defined Debye temperature Θ_S . In *ab initio* calculations one has successfully related E_{coh} to the detailed electron band structure, but only for elemental solids¹ and simple compounds.² Miedema's formula³ offers a semiempirical account of $\Delta^0 H$ which is related to the electronic structure of the constituent elements, but does not refer to the electron band structure of the compound. Vibrational frequencies have been calculated by *ab initio* methods for specific phonon modes in simple systems⁴ or in the elastic limit (e.g., bulk modulus), but very little has been done on Θ_S in compounds.

One demanding task regarding cohesive properties is the calculation of phase diagrams of alloys. Two very different approaches have been taken: *ab initio* calculations based on the electron band structure, and CALPHAD ("calculation of phase diagrams") work,⁵ which is the coupling of thermochemical data and computer cal-

culation of phase diagrams. The first method usually leaves out the vibrational part of the Gibbs energy. The CALPHAD method rests on experimental data for the total Gibbs energy, without regard to their microscopic origin (e.g., electronic and vibrational). Considerable progress in the calculation of phase diagrams could be achieved if the CALPHAD method is complemented by reliable information on $G(T)$ from basic solid-state physics. In particular, this refers to metastable phases, i.e., for phases whose properties are not known from experiments.

It is the purpose of this paper to establish a method to find the vibrational Gibbs energy of compounds. We shall base it on three parameters: the average number of valence electrons per atom in the compound (n_e), the average volume per atom (Ω), and the logarithmically averaged atomic mass (M_{eff}).

Our method turns out to be widely applicable. Here we shall treat two main groups of compounds: (1) 3d transition-metal compounds MX in the NaCl structure, where $X = \text{C, N, O}$ or S , and (2) 3d transition-metal carbides and nitrides of complex crystal structure and with metallic character. As an illuminating application, we discuss phase diagrams with possible metastable phases. Further, we estimate standard entropies $^0 S$ and enthalpies of formation $\Delta^0 H$ for a large number of compounds where experiments or other estimates are lacking or uncertain.

The outline of the paper is as follows. In Sec. II we introduce a quantity E_S with the dimension of energy which is closely related to the entropy Debye temperature Θ_S . Section III, devoted to the NaCl structure, establishes relations between n_e and the three quantities E_{coh} , E_S , and $\Delta^0 H$, and gives an interpretation of the empirical results in terms of the electron band structure. In Sec. IV we extend the E_S - n_e and $\Delta^0 H$ - n_e relations to carbides and nitrides of complex structure. A general scheme of analysis, based on our relations, is introduced in Sec. V, and applied in Sec. VI to phase-stability problems and in Sec. VII to the estimation of, e.g., Θ_S , 0S , and $\Delta^0 H$.

II. A CHARACTERISTIC ENERGY E_S RELATED TO LATTICE VIBRATIONS

The derivation of an effective force constant k_S from thermal data has been dealt with previously,⁶⁻⁹ and we only give the main points. For a single harmonic oscillator, the frequency ω is related to the mass M and the force constant k by $\omega^2 = k/M$. In a real solid, one has a spectrum of vibrational frequencies. The entropy at high temperatures measures the logarithmically averaged frequency. Therefore, we can define an entropy-related

effective force constant by $k_S = M_{\text{eff}}(k_B \Theta_S / \hbar)^2$. M_{eff} is the logarithmically averaged mass of the compound, and Θ_S is an entropy Debye temperature,¹⁰ i.e., the Θ value that gives the experimental vibrational entropy $S_{\text{vib}}(T)$ if Θ_S is inserted in the Debye-model expression S_D for the entropy,

$$S_{\text{vib}}(T) = S_D(\Theta_S/T). \quad (1)$$

At low temperatures ($T \ll \Theta_S$), $\Theta_S(T)$ varies with T because the true spectrum is not of the Debye form, and at high temperatures ($T > \Theta_S$), it decreases with T because of anharmonic effects. To get a stable value for Θ_S (and hence for k_S), we evaluate Θ_S at $T \approx \Theta_S$.

Before Θ_S can be calculated from the total experimental entropy, nonvibrational contributions (electronic, magnetic, etc.) should be subtracted. We have neglected these contributions, except for the electronic entropy of the compound TiN which was estimated⁷ as $S_{\text{el}} = \gamma_0 T$.

Using experimental data on the entropy, S , and the volume per atom, Ω , we calculate Θ_S , the related effective force constant k_S , and the characteristic energy $E_S = k_S \Omega^{2/3}$, as in Tables I and II. The tables also give the crystal structure, the average number of valence electrons per atom (n_e), and the quantity n_e/Ω . As an illustration, a compound M_3X_2 would have $n_e =$

TABLE I. Properties of compounds with the NaCl (cF8) structure.

Compound	Θ_S (K)	k_S (N/m)	Ω (10^{-30} m ³ /atom)	n_e (e/a)	n_e/Ω (10^{30} e/m ³)	E_S (Ry)	$\Delta^0 H$ (kJ/mol of atoms) ¹
ScC	654 ^a	283	13.144 ^b	3.5	0.266	7.230	a
ScN	755 ^c	407 ^c	11.429 ^b	4	0.350	9.480 ^c	-220 ^c
ScO	670 ^c	343 ^c	11.015 ^b	4.5	0.409	7.800 ^c	-326 ^c
ScS	483 ^c	252 ^c	17.492 ^b	4.5	0.257	7.800 ^c	k
TiC	805 ^d	442	10.110 ^e	4	0.396	9.480	f
TiN	710 ^d	372	9.521 ^e	4.5	0.473	7.666	f
TiO	613 ^f	296	9.144 ^e	5	0.547	5.938	f
VC	745 ^d	391	9.058 ^e	4.5	0.497	7.794	j
VN	631 ^d	303	8.869 ^e	5	0.564	5.955	f
VO	535 ^f	233	8.741 ^e	5.5	0.629	4.535	f
CrC ^g	664 ^c	314 ^c	8.700 ^c	5	0.575	6.100 ^c	-10 ^c
CrN ^h	535 ^c	220 ^c	8.921 ^b	5.5	0.616	4.35 ^c	f
CrO ^g	409 ^c	137 ^c	8.615 ⁱ	6	0.696	2.650 ^c	-160 ^c
MnC ^g	557 ^c	227 ^c	8.700 ^c	5.5	0.632	4.400 ^c	Sec. VIB
FeC ^g	434 ^c	139 ^c	8.500 ^c	6	0.706	2.650 ^c	Sec. VIC

^aFrom high-temperature data in Ref. 61.

^bFrom lattice-parameter data in Ref. 62.

^cPresent estimate, discussed in the text.

^dReferences 6-8.

^eFrom lattice-parameter data quoted in Ref. 2.

^fReference 53.

^gMetastable modification.

^hHigh-temperature modification. A comparison with values from Ref. 53 is given in the text.

ⁱFrom lattice-parameter data in Ref. 63.

^jReference 55.

^kProperty under study. To be considered in forthcoming papers.

¹Our estimate or reference to data used by us.

TABLE II. Properties of complex compounds.

Compound	Θ_S (K)	k_S (N/m)	Ω (10^{-30} m ³ /atom)	n_e (e/a)	n_e/Ω (10^{30} e/m ³)	E_S (Ry)	Δ^0H (kJ/mol of atoms) ^p
Sc ₂ C (<i>hR3</i>)	465 ^a	178	17.246 ^d	3.33	0.193	5.451	a
Sc ₄ C ₃ (<i>cI28</i>)	531 ^a	205	13.369 ^d	3.43	0.256	5.297	a
Cr ₂₃ C ₆ (<i>cF116</i>)	o	o	10.413 ^b	5.59	0.537	o	f
Cr ₃ C (<i>oP16</i>) ^g	502 ^c	259 ^c	9.966 ^b	5.50	0.552	5.500 ^c	−12 ^c
Cr ₃ C ₂ (<i>oP20</i>)	609 ^f	305	8.978 ^b	5.20	0.579	6.044	f
Cr ₇ C ₃ (<i>hP80</i>)	537 ^f	275	9.569 ^b	5.40	0.564	5.686	f
Cr ₂ N (<i>hP9</i>)	445 ^c	189 ^c	9.894 ^b	5.67	0.573	4.000 ^c	f
Mn ₇ C ₃ (<i>oP40</i>)	479 ^c	227	9.472 ^b	6.10	0.644	4.662	e
Mn ₅ C ₂ (<i>mC28</i>)	468 ^c	222	9.642 ^b	6.14	0.637	4.613	e
Mn ₃ C (<i>oP16</i>)	440 ^c	207	9.838 ^b	6.25	0.635	4.360	e
Mn ₂₃ C ₆ (<i>cF116</i>)	431 ^c	212	10.355 ^b	6.38	0.616	4.620	e
Mn ₂ N (<i>hP3</i>)	372 ^c	137 ^c	10.380 ^b	6.33	0.610	3.000 ^c	−31.0 ^c
Mn ₅ N ₂ (hex)	357 ^c	135 ^c	10.180 ^h	6.43	0.632	2.900 ^c	m
Mn ₄ N (<i>cP5</i>) ^h	314 ^c	117 ^c	11.646 ^h	6.60	0.567	2.750 ^c	m
Fe ₂ C (<i>hP3</i>)	445 ^c	189 ^c	9.517 ^b	6.67	0.701	3.900 ^c	3.5 ^c
Fe ₇ C ₃ (<i>oP40</i>)	432 ^c	187 ^c	9.324 ^b	6.80	0.729	3.800 ^c	4.5 ^c
Fe ₅ C ₂ (<i>mC28</i>)	431 ^c	190 ^c	9.467 ^b	6.86	0.725	3.900 ^c	5.0 ^c
Fe ₃ C (<i>oP16</i>)	394 ⁱ	168	9.702 ^b	7.00	0.722	3.506 ^c	i
Fe ₂ N (<i>hP3</i>)	338 ^j	115	9.243 ^b	7.00	0.757	2.323	n
Fe ₄ N (<i>cP5</i>)	300 ^j	108	10.948 ^b	7.40	0.676	2.443	m
Co ₂ C (<i>oP6</i>)	411 ^c	167 ^c	9.383 ^b	7.33	0.781	3.400 ^c	7.0 ^c
Co ₃ C (<i>oP16</i>)	386 ^k	168	9.492 ^b	7.75	0.816	3.455	k
Co ₂ N (<i>oP6</i>)	321 ^c	107 ^c	9.515 ^b	7.67	0.806	2.200 ^c	−1.0 ^c
Co ₃ N (<i>hP8</i>) ^h	292 ^c	100 ^c	9.981 ^b	8.00	0.802	2.130 ^c	0.0 ^c
Co ₄ N (<i>cP5</i>)	276 ^c	96 ^c	10.446 ^b	8.20	0.785	2.100 ^c	0.5 ^c
Ni ₃ C (<i>oP16</i>) ^g	338 ^l	128	9.220 ^c	8.50	0.922	2.582	l
Ni ₃ N (<i>hP8</i>) ^h	288 ^c	97 ^c	9.889 ^b	8.75	0.885	2.050 ^c	g
Ni ₄ N (<i>cP5</i>)	272 ^c	93 ^c	10.463 ^b	9.00	0.860	2.050 ^c	1.0 ^c

^aFrom high-temperature data in Ref. 61.^bFrom lattice-parameter data in Ref. 62.^cPresent estimate, discussed in the text.^dReference 64.^eReference 40.^fReference 53.^gMetastable modification.^hReference 65.ⁱReference 42.^jReference 66.^kReference 67.^lReference 68.^mReference 55.ⁿReference 69.^oProperty under study. To be considered in forthcoming papers.^pOur estimate, or reference to data used by us.

$(3n_M + 2n_X)/5$. Here n_M and n_X are the number of valence electrons for atoms M and X .

The entropy at $T = 298.15$ K, i.e., the standard entropy 0S , is given here in the unit J/K mol of atoms. For instance, 0S is $\frac{1}{5}$ of the entropy per mole of formula units of a compound M_3X_2 . This definition of 0S allows a simple and meaningful comparison of compounds with different numbers of atoms per formula unit.

The enthalpy of formation Δ^0H is defined in analogy to

0S , evaluated at room temperature and expressed in kJ/mol of atoms. E_S is an energy per atom. Because it is compared with E_{coh} from *ab initio* work, we choose to give it in rydbergs (1 Ry/atom = 1312.8 kJ/mol).

For later reference, we note Latimer's rule^{11,12} for the estimation of 0S of a compound. It relies on the strong atomic-mass influence on Θ_S , but treats the interatomic forces in a crude way, without connection to the electron band structure.

III. RESULTS FOR COMPOUNDS WITH NaCl STRUCTURE

A. Relation between E_S and E_{coh}

Figure 1 shows our E_S versus the cohesive energy E_{coh} calculated by Zhukov *et al.*² as the difference between the total energies of the free atoms and the total energy per unit cell of TiC, VC, TiN, VN, TiO, and VO. These compounds all have the NaCl (*cF8*) structure. There is conflicting information on the cohesive energy of VC. Zhukov *et al.* analyzed experimental data on the enthalpy change of the reaction $MX(s) = M(g) + X(g)$ at 298 K, which is the experimental analogue of their E_{coh} , and concluded that they imply $(E_{\text{coh}})_{\text{TiC}} < (E_{\text{coh}})_{\text{VC}}$, while their own calculation gave the reversed inequality. Results from Brewer and Krikorian¹³ agree with the theoretical trend of Zhukov *et al.* The theoretical trend is also supported by our results in Figs. 1 and 2.

Figure 1 demonstrates that E_S is a useful quantity and a complement to E_{coh} in a study of the cohesive properties of solids. This is of practical importance since experimental data on E_{coh} are often uncertain or lacking because they rest on difficult high-temperature experiments. 0S , from which E_S can be obtained, may be easier to measure. In fact, Zhukov *et al.* had to rely on their own theoretical E_{coh} when they related it to n_e . In the rest of this paper we shall deal with E_S , but not with E_{coh} .

B. Relation between E_S and n_e for compounds with NaCl structure

Figure 2 shows E_S versus n_e for various metallic carbides, nitrides, and oxides with $3.5e/a \leq n_e \leq 5.5e/a$, which crystallize in the NaCl structure. A plot of the negative enthalpy of formation at 298 K ($-\Delta^0H$) shows a similar trend, Fig. 3, although different relations are obtained for Δ^0H of carbides, nitrides, and oxides.

C. Bonding and the electron band structure of compounds with NaCl structure

Part of Fig. 2 refers to the range $4e/a \leq n_e \leq 5.5e/a$ where Zhukov *et al.*² found a linear decrease of E_{coh} with increasing n_e . The decrease can be understood from the following theoretical argument. Figure 4 gives the gross features of the electron density of states $N(E)$ for TiC, as calculated by Zhukov *et al.*² and Neckel *et al.*¹⁴ The large bonding energy arises in TiC because the Fermi level E_F falls in a pronounced gap in $N(E)$ which separates bonding and antibonding electron states.^{14,15} The decrease in E_{coh} and E_S with increasing n_e is due to antibonding states being filled. Further, when $n_e < 4e/a$ not all the bonding states are filled¹⁶ and E_{coh} is expected to decrease. Zhukov *et al.*² did not consider this case, but the prediction is confirmed by the present analysis of the experimental information on E_S (Fig. 2) and Δ^0H (Fig. 3) of ScC.

Schwarz¹⁵ has reviewed the relation between bonding

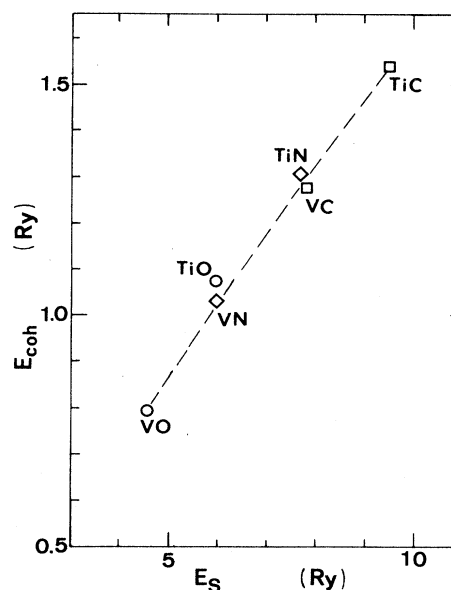


FIG. 1. The quantity $E_S \equiv k_S \Omega^{2/3}$ correlates well with the cohesive energy E_{coh} , calculated by Zhukov *et al.* (Ref. 2). Here k_S is an effective interatomic force constant derived from experimental data on the vibrational entropy. Ω is the average volume per atom. The dashed line is to guide the eye.

and the electronic band structure in refractory compounds. The relation between the band structure and the relative stability of several (*p-d*)-bonded structures has been discussed by Pettifor and Podloucky.¹⁷ Although,

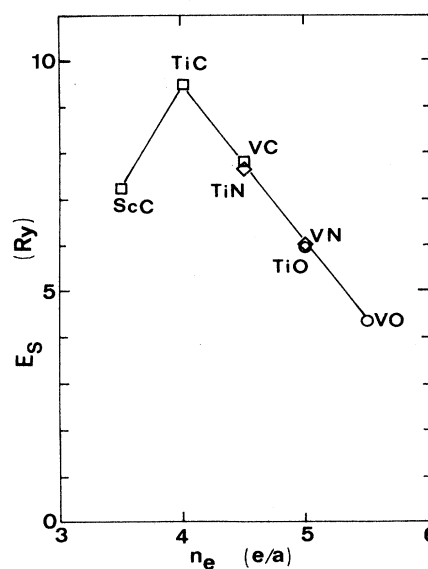


FIG. 2. E_S vs n_e , the average number of valence electrons per atom, for MX compounds ($X = \text{C, N, O}$) with the NaCl (*cF8*) structure.

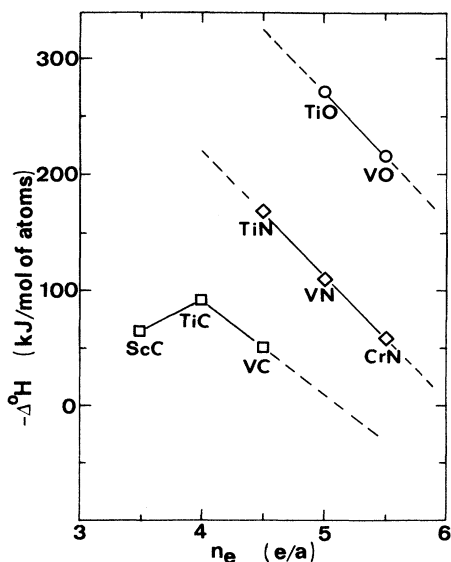


FIG. 3. The enthalpy of formation $\Delta^0 H$ of (cF8) compounds MX ($X = C, N, O$) at 298 K, vs n_e . The dashed lines are used to extrapolate the experimental data in Secs. VI and VII.

as a first approximation, one may adopt a rigid-band picture, atomic-size effects¹⁸ related to the nonmetal atoms also seem to be important. Several papers deal with the bonding and electronic structure in specific compounds, e.g., TiC_xN_{1-x} ,¹⁹ TiC ,²⁰ ScN and TiC ,²¹ and ScC and ScN .¹⁶

IV. EXTENSION OF THE $E_S - n_e$ AND $\Delta^0 H - n_e$ RELATIONS: LARGE n_e VALUES AND COMPLEX STRUCTURES

A. General considerations

The previous section showed a remarkably good correlation between E_S and n_e for several compounds of the NaCl structure, a fact which was also given a theoretical interpretation in terms of the electron band structure.

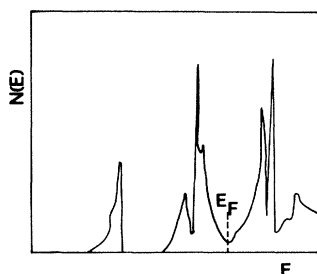


FIG. 4. The gross features of the electron density of states $N(E)$ for TiC (arbitrary units). The Fermi level falls in a gap between bonding and antibonding states.

We shall now see that the $E_S - n_e$ and $\Delta^0 H - n_e$ relations can be extended to compounds of more complex structures and to systems with n_e outside the range considered in Sec. III. However, correlations of the type discussed in this work can only be expected to hold when one stays within a group of compounds with similar bonding, i.e., similar electronic band structure. In this paper we shall focus on complex carbides and nitrides which have some metallic character. The monoxides MnO , FeO , CoO , and NiO (NaCl or distorted NaCl structure) are antiferromagnetic insulators at low temperatures²² with an electronic structure which has been difficult to account for. They will be the subject of separate studies, following the general ideas of this paper. Elsewhere, we will also treat M_2O_3 and M_3O_4 oxides, which include magnetic systems and metal-insulator transitions, as well as sulfides, borides, and phosphides. Of particular interest, and to be discussed in a separate paper, are MX compounds with the $NiAs$ (hP4) structure. They have octahedrally coordinated cations, like the NaCl structure, and differ only in the anion stacking. VS ($n_e = 5.5e/a$) and CrS ($n_e = 6e/a$) have high-temperature (hP4) metallic modifications. Their E_S lie on the straight line for the NaCl structure in Fig. 2. We shall refer to this fact in Sec. VII when we estimate the properties of ScS .

In a comparison of compounds with the same crystal structure, n_e is a natural parameter. When compounds of different structures are compared it might be better to correlate to, e.g., the average valence-electron density per volume Ω . One may then use various definitions of Ω , such as unit-cell volume or average volume per atom. We found that alternative definitions of n_e , or of Ω in the complex structures, did not improve the correlations, and in some cases made them poor.

B. Complex carbides and nitrides: $E_S - n_e$ and $\Delta^0 H - n_e$

Table II lists carbides and nitrides of more complex structure than NaCl. The E_S data for carbides are plotted in Fig. 5(a) versus n_e . Two scandium carbides give information on E_S for $n_e < 3.5$ (i.e., the lowest limit in Fig. 2), Sc_2C (hR3) with $n_e = 3.33e/a$ and Sc_4C_3 (cI28) with $n_e = 3.43e/a$. The corresponding data points in Fig. 5(a) suggest that when $n_e < 4e/a$, E_S decreases with n_e also for the more complex structures. A similar result is shown by the $E_S - n_e$ data on borides.²³

Figure 5(b) gives $\Delta^0 H$ of carbides versus n_e . The manganese carbides deviate somewhat from the trend of the other compounds. This is significant and expected, because $\Delta^0 H$ depends in part on the bonding of the constituent elements. It is well known that the $E_{coh} - n_e$ relation for transition metals shows an anomalously low value for Mn. That is reflected in a high $\Delta^0 H$ of Mn compounds. E_S , on the other hand, depends only on the bonding in the compound and not on that of the constituent elements. Therefore, we do not expect anomalies in E_S for Mn compounds, in agreement with Fig. 5(a).

The thermodynamic information on the entropy of nitrides is scarce, and our $E_S - n_e$ curve [Fig. 6(a)] should be considered as tentative at large n_e . The $\Delta^0 H - n_e$ plot for

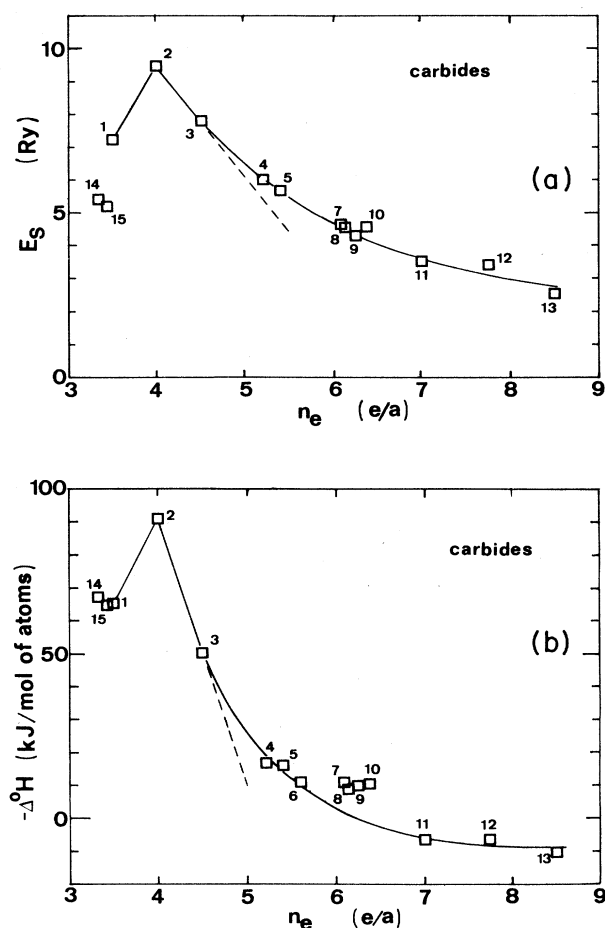


FIG. 5. (a) E_S and (b) Δ^0H of carbides, as functions of n_e . The numbers refer to (1) ScC, (2) TiC, (3) VC, (4) Cr_3C_2 , (5) Cr_7C_3 , (6) Cr_{23}C_6 , (7) Mn_7C_3 , (8) Mn_5C_2 , (9) Mn_3C , (10) Mn_{23}C_6 , (11) Fe_3C , (12) Co_3C , (13) Ni_3C , (14) Sc_2C , (15) Sc_4C_3 , with identical identification for the E_S values at the same n_e . The dashed lines refer to the (cF8) structure.

nitrides [Fig. 6(b)] shows a dependence on n_e similar to that found for carbides. The manganese nitrides deviate from the general trend, in line with the previous discussion.

Very little is known about the electronic band structure of the complex carbides and nitrides considered here.²⁴ In view of the crudeness to describe a complicated band structure in terms of essentially only one parameter (n_e), the correlations found are most remarkable.

V. A GENERAL SCHEME OF ANALYSIS

A. Estimation procedure for Θ_S , 0S , and Δ^0H

In the subsequent application of the first part of this paper, the following procedure is used. From an assumed ideal stoichiometry of a compound M_mX_n we calculate n_e . The number of valence electrons per 3d transition metal ranges from three (Sc) to 10 (Ni), and for the non-

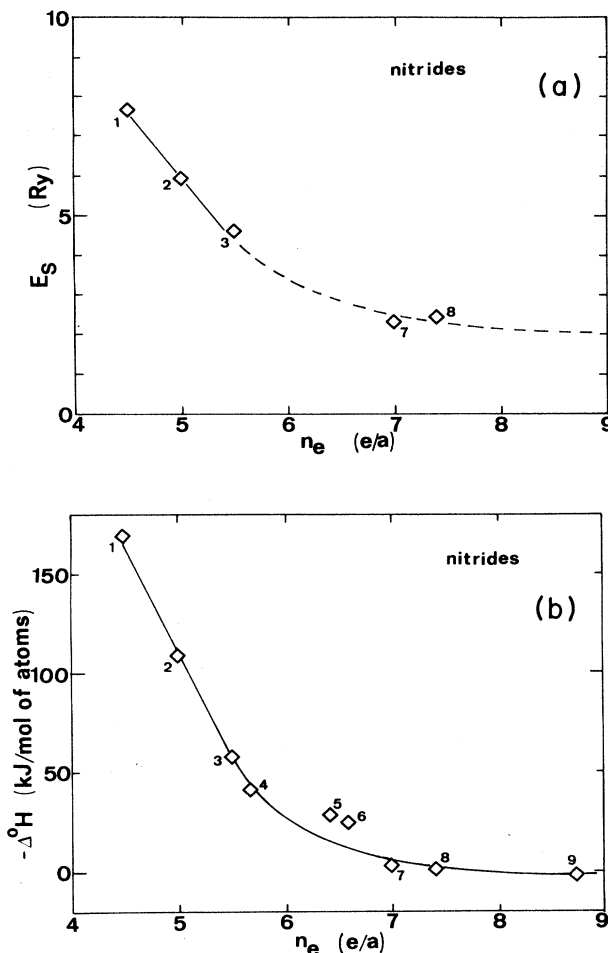


FIG. 6. (a) E_S and (b) Δ^0H of nitrides, as in Fig. 5. The numbers refer to (1) TiN, (2) VN, (3) CrN, (4) Cr_2N , (5) Mn_3N_2 , (6) Mn_4N , (7) Fe_2N , (8) Fe_4N , and (9) Ni_3N . The E_S - n_e relation is only tentative.

metals we take four (C), five (N), and six (O,S). We next assume that E_S (and Δ^0H) can be estimated from a recommended line in the corresponding E_S - n_e (Δ^0H - n_e) plot. In some cases [part of Fig. 3 and Fig. 6(a)] the experimental data are too few to firmly establish the solid or dashed lines. However, the better founded and analogous trends in other plots, and the general relationship observed between E_S , Δ^0H and E_{coh} , lends support to the suggested relations in Figs. 3 and 6(a). From data on the lattice parameters, we get Ω . Then k_S and Θ_S are derived from $E_S = k_S \Omega^{2/3}$, which finally allows us to estimate 0S . Anharmonicity makes Θ_S temperature dependent (a decrease by, say, 10–20% from $T = \Theta_S$ to the melting temperature). When the vibrational entropy at high temperatures is needed, we let Θ_S vary with T . Just as E_S and Δ^0H show a regular variation with n_e , so does the anharmonic softening in Θ_S , and we rely on the known behavior of the temperature dependence of $\Theta_S(T)$ for similar compounds. Usually, $\Theta_S(T)$ varies little in

the range $\Theta_S/3 < T < \Theta_S$, which makes our estimate of 0S quite accurate even when $\Theta_S > 298$ K.

When experimental data for the molar volume Ω are available, an explicit reference is given in Tables I and II. For metastable phases, we assume that their n_e/Ω is the same as for the stable ones. If no other information on Ω for a particular compound is available, we rely on extrapolations or interpolations in Ω - n_e plots, which have been found to show a high degree of regularity.

The uncertainties given for E_S , Θ_S , 0S , and Δ^0H are our estimates and reflect the typical spread in the correlations on which the analysis is based, including the uncertainty in Ω of the metastable phases. The measured 0S used to establish our correlation is not corrected for the electronic part of the entropy (except for TiN). Therefore, our Θ_S may systematically be slightly low. However, this also means that an average electronic entropy is included in the 0S values we obtain from Θ_S , and it would not be correct to add an electronic term obtained from, e.g., band-structure work.

Some of the compounds considered in Sec. III show magnetic transitions at critical temperatures $T_c > 298$ K. That is expected to increase the entropy above the value given by our Θ_S , when $T > T_c$.

B. Coupling with the CALPHAD work

We shall repeatedly refer to the results of the so-called CALPHAD (Ref. 5) (i.e., "calculation of phase diagrams") work on alloy systems. It involves the coupling of phase-diagram and thermochemical data using models for the Gibbs energy of various individual phases. The use of computer-optimization techniques²⁵ allows the CALPHAD-type analysis (so-called CALPHAD assessments²⁶) to produce a consistent description of the thermodynamics of the system, which is often more reliable than the results of a single experimental study. In this paper, CALPHAD work is often relied on. We use the results of CALPHAD assessments in cases where experimental data are lacking (e.g., Co_3C , Ni_3C , and Fe_2N). Further, we compare our predictions for some metastable phases with CALPHAD-type extrapolations from higher-order systems (e.g., for Cr_3C). Finally, our predictions are used as input in phase-diagram calculations²⁷ to get new insight in the stability of the NaCl structure for compounds with a large n_e (Sec. VI).

VI. PHASE STABILITY OF CARBIDES WITH THE NaCl STRUCTURE AS A FUNCTION OF n_e

In the interval $4e/a \leq n_e \leq 5.5e/a$, experimental data show that E_S , and hence Θ_S , for MX compounds of the NaCl structure decreases (Fig. 2). A similar behavior is found for $-\Delta^0H$ (Fig. 3). The trend in Δ^0H implies a destabilization of the NaCl phase at low temperatures. However, the simultaneous decrease in Θ_S may make that phase stable at high temperatures through the increased entropy S in the Gibbs energy $G = H - TS$.

Hägg,²⁸ long ago, noted that the complex carbide structures are favored when n_e increases along the d

series. Here we shall include temperature effects in an investigation of the relative stability of CrC, MnC, and FeC.

A. The CrC (NaCl) phase; $n_e = 5e/a$

1. Analysis of molar-volume data

A carbide with the approximate composition "CrC" was early reported²⁹ as a high-temperature phase in the Cr-C system, but its crystal structure was not determined. The possibility that it has the NaCl (*cF8*) structure is discussed in more recent compilations,^{30,31} and the lattice parameter $a_0 = 3.61 \times 10^{-10}$ m is given by assuming that the "CrC" phase corresponds to the NaCl carbide found by Goldschmidt³² in chromium steels (which he called Ψ -carbide). This assumption, and the phase stability of "CrC," will now be examined by combining the methods of this paper with detailed phase-diagram calculations. First, we note that the experimental n_e/Ω for the stable chromium carbides (Cr_3C_2 , Cr_7C_3 , and Cr_{23}C_6) fall in a narrow range. Their average $(n_e/\Omega)_{\text{av}} = [0.56(\pm 0.02)] \times 10^{30} \text{ e/m}^3$ is close to that of the metastable Cr_3C (*oP16*) (Sec. VII B 2). Assuming a similar behavior for the "CrC" phase, with $n_e = 5e/a$, we predict $\Omega = \{5/[0.56(\pm 0.02)]\} \times 10^{-30} = [8.9(\pm 0.3)] \times 10^{-30} \text{ m}^3/\text{atom}$. An extrapolation in the Ω - n_e plot for NaCl carbides gives $\Omega = [8.7(\pm 0.2)] \times 10^{-30} \text{ m}^3/\text{atom}$. These estimated volumes, and the reported a_0 , give $N = a_0^3/\Omega = [5.4(\pm 0.2)] \text{ atoms/cell}$ for "CrC," which is significantly lower than $N = 8$ of the NaCl (*cF8*) structure. Therefore, we consider it unlikely that a_0 corresponds to the formula "CrC." Alternatively, we estimate the number of electrons per cell of the Ψ -carbide as $(a_0)^3(n_e/\Omega)_{\text{av}} = 26.3 \text{ e/cell}$ and combine this value with the result of the chemical analysis for the two carbide samples (9.04 wt. % C and 8.4 wt. % C) reported in Ref. 32. That gives formulas which can be written as $\text{Cr}_7\text{C}_{3.14}$ and $\text{Cr}_7\text{C}_{2.89}$, respectively. This suggests that Goldschmidt's data refer to the Cr_7C_3 (*hP80*) carbide, which is stable in the Cr-C and the Fe-Cr-C systems. We shall, therefore, not use the reported a_0 in the subsequent analysis of the stability of the NaCl structure in the Cr-C system, but take $\Omega = [8.7(\pm 0.3)] \times 10^{-30} \text{ m}^3/\text{atom}$, cf. above.

2. Gibbs energy and calculation of the phase diagram

From the correlation in Fig. 2 [i.e., the dashed line in Fig. 5(a)], $E_S = 6.1 \text{ Ry}$ for CrC ($n_e = 5e/a$). With our selected Ω this gives $k_S = [314(\pm 8)] \text{ N/m}$ and $\Theta_S = [664(\pm 9)] \text{ K}$, and an estimated entropy at $T \approx \Theta_S$, $S(664 \text{ K}) = [33.87(\pm 0.3)] \text{ J/K mol of atoms}$. Further, a linear extrapolation in Fig. 5(b) gives $\Delta^0H = -10 \text{ kJ/mol of atoms}$. With these estimates, thermodynamic information on Cr (Ref. 33) and C (Ref. 34), and the assumption that the anharmonic softening of Θ_S is similar to that of the stable Cr carbides, we fit the Gibbs energy to $G(T) = a + bT + cT \ln T + dT^2 + e/T$, as discussed in Ref. 35. Phase-diagram calculations performed by combining

$G(T)$ for CrC with a recent³⁶ thermodynamic description of the stable phases in the Cr-C system suggest that CrC is metastable at all temperatures. This is in agreement with experiments³⁷ where the CrC phase could not be detected up to 2000°C. However, we find that a change in Δ^0H to -11 kJ/mol of atoms is enough to stabilize it above 1500 K,³⁸ showing that the NaCl structure is relatively close to being stable in the Cr-C system.

B. The MnC (NaCl) phase; $n_e = 5.5e/a$

No carbide with the NaCl structure has been found in the Mn-C system. This fact is also in line with the rapid destabilization of this structure with increasing n_e , Figs. 5(a) and 5(b). A more precise prediction of the lattice stability of the MnC (cF8) phase is hampered by the lack of information for extrapolating the $\Delta^0H - n_e$ relation to MnC, i.e., to $n_e = 5.5e/a$. Nevertheless, an approximate analysis will show that the maximum destabilizing effect predicted by our correlations is enough to make MnC (cF8) a metastable phase.

We estimate $\Omega(\text{MnC}) = [8.7(\pm 0.1)] \times 10^{-30}$ m³/atom from the average $(n_e/\Omega)_{\text{av}} = [0.63(\pm 0.01)] \times 10^{30}$ e/m³. The correlation in Fig. 2 gives $E_S = 4.40$ Ry, $k_S = [227(\pm 2)]$ N/m, and $\Theta_S = [557(\pm 3)]$ K. We use Θ_S (with allowance for an anharmonic softening at high T), available descriptions of C,³⁴ Mn,³⁹ and the stable phases in the Mn-C system⁴⁰ and calculate the phase diagram for various Δ^0H . We found that MnC (cF8) does not appear as a stable phase when $\Delta^0H \geq -3.6$ kJ/mol of atoms, whereas a linear extrapolation in the $\Delta^0H - n_e$ diagram (suggested, e.g., by the $\Delta^0H - n_e$ data for NaCl nitrides in Fig. 3) gives, for the most positive Δ^0H , a significantly larger value, $\Delta^0H = 30$ kJ/mol of atoms.

C. The FeC (NaCl) phase; $n_e = 6e/a$

In the discussion above on the maximum destabilizing effect upon Δ^0H for MnC we relied on a linear extrapolation in the $E_S - n_e$ and $\Delta^0H - n_e$ plots. That seems justified by the experimental data on various compounds with the NaCl structure (Figs. 2 and 3). For $n_e = 6e/a$, however, no experimental data are available and we must consider the possibility of a nonlinear $\Delta^0H - n_e$ plot with positive deviation. That would imply a smaller destabilizing effect than implied by the value $\Delta^0H = 70$ kJ/mol of atoms given by the straight dashed line in Fig. 5(b).

From a consideration of $(n_e/\Omega)_{\text{av}} = [0.72(\pm 0.01)] \times 10^{30}$ e/m³ and trends in the $\Omega - n_e$ plot for (cF8) MX compounds, we estimate $\Omega(\text{FeC}) = [8.5(\pm 0.2)] \times 10^{-30}$ m³/atom. Then, with the correlation in Fig. 2, $E_S = 2.65$ Ry, $k_S = [139(\pm 2)]$ N/m, and $\Theta_S = [434(\pm 3)]$ K. Finally, we use Θ_S at high temperatures, with allowance for anharmonic softening, information on the properties of Fe,⁴¹ C,³⁴ and the Fe-C system⁴² and calculate the Fe-C phase diagram for several choices of Δ^0H for FeC. Then, we find that already for $\Delta^0H \geq 22$ kJ/mol of atoms, FeC (NaCl) does not appear as a stable phase in the Fe-C phase diagram. We conclude that the destabilization of FeC (NaCl) is possible even when there is an appreciable

nonlinearity in the $\Delta^0H - n_e$ curve. This corroborates the fact that a NaCl carbide with the composition FeC has not been found. An early report on "FeC" by Eckstrom and Adcock⁴³ was later shown⁴⁴ to correspond to Fe₇C₃.

VII. APPLICATION: ESTIMATION OF THE ENTROPY DEBYE TEMPERATURE Θ_S AND THE ENTHALPY OF FORMATION Δ^0H FOR 3d-TRANSITION-METAL COMPOUNDS

A. Scandium compounds

1. ScN (cF8)

No experimental data on the entropy of ScN seem to be available. ScN has the same n_e ($4e/a$) and the same crystal structure (NaCl) as TiC which, by Fig. 2, suggests that $E_S(\text{ScN}) = E_S(\text{TiC})$. This gives $k_S = [407(\pm 9)]$ N/m and $\Theta_S = [755(\pm 9)]$ K. Then $^0S = [14.0(\pm 0.5)]$ J/K mol of atoms, which may be compared with $^0S = [14.8(\pm 2)]$ J/K mol of atoms from Kubaschewski and Alcock.⁴⁵ The correlation in Fig. 2 is better than implied by the uncertainties in their estimate, which makes our approach a valuable complement to other methods of estimating 0S when experimental information is uncertain or lacking.

There is no direct experimental information on Δ^0H for ScN, but the following estimates have been presented (in kJ/mol of atoms): -154 ,^{46,47} -141 ,⁴⁸ and -184 .³ A linear extrapolation in Fig. 3 to $n_e = 4e/a$ gives $\Delta^0H = -220$ kJ/mol of atoms, which is larger than obtained in previous works.

2. ScO (cF8)

There seem to be no estimates of the thermodynamic properties of ScO ($n_e = 4.5e/a$). From Fig. 2 we get $E_S(\text{ScO}) = [7.8(\pm 0.2)]$ Ry which, combined with the experimental Ω , gives $k_S = [343(\pm 9)]$ N/m, $\Theta_S = [670(\pm 9)]$ K, and hence, $^0S = [16.0(\pm 0.3)]$ J/K mol of atoms. A linear extrapolation in Fig. 3 yields $\Delta^0H = -326$ kJ/mol of atoms.

3. ScS (cF8)

The correlation in Fig. 2 does not contain any experimental data for sulfides. However, since a common relation is found for carbides, nitrides, and oxides, and since VS and CrS (in the NiAs structure) also fit the trend,²³ we tentatively apply the result of Fig. 2 to ScS. Then, for $n_e = 4.5e/a$, we get $E_S = [7.8(\pm 0.2)]$ Ry, $k_S = [252(\pm 7)]$ N/m, $\Theta_S = [483(\pm 7)]$ K, and hence, $^0S = [23.0(\pm 0.3)]$ J/K mol of atoms. Mills,⁴⁹ using Latimer's rule, estimated $^0S = [28.24(\pm 4)]$ J/K mol of atoms.

B. Chromium compounds

1. CrC (cF8)

The properties of CrC are discussed in Sec. VI A.

2. Cr_3C (*oP16*)

The “cementite” phase M_3C (*oP16*) forms in Fe-C and Fe-Cr-C alloys, but is metastable in the Cr-C system. Recently, Cr_3C has been obtained by splat quenching of liquid binary alloys.⁵⁰ Its thermodynamic properties are not known. Using the measured Ω and Fig. 5(a) with $n_e = 5.5e/a$, we get $E_S = [5.5(\pm 0.2)]$ Ry, $k_S = [259(\pm 10)]$ N/m, and $\Theta_S = [502(\pm 10)]$ K, from which $^0S = [22.0(\pm 0.5)]$ J/K mol of atoms. This may be compared with $^0S = 23.6$ J/K mol of atoms obtained from a recent description⁵¹ of the thermodynamic properties of the cementite phase in Fe-Cr-C, $(\text{Fe,Cr})_3\text{C}$.

From Fig. 5(b) we estimate $\Delta^0H = [-12(\pm 2)]$ kJ/mol of atoms, which compares well with an estimate from Miedema's formula,³ $\Delta^0H = -11$ kJ/mol of atoms. From the description⁵¹ of $(\text{Fe,Cr})_3\text{C}$ we get $\Delta^0H = -9.92$ kJ/mol of atoms.

3. CrN (*cF8*)

CrN crystallizes in the (*cF8*) structure at high temperatures, but undergoes a transition to the orthorhombic structure (*oP4*) below $T \approx 285$ K,⁵² which is associated with a paramagnetic to antiferromagnetic transition. From the correlation in Fig. 2 we predict that for the high-temperature metallic (*cF8*) phase, $E_S = [4.35(\pm 0.2)]$ Ry, $k_S = [220(\pm 10)]$ N/m, and $\Theta_S = [535(\pm 12)]$ K. This gives, e.g., at $T = 500$ K, $S(500) = [32.3(\pm 0.5)]$ J/K mol of atoms, to be compared with $S(500) = 31.4$ J/K mol of atoms from the JANAF Tables.⁵³ [E_S derived from JANAF's tables is represented in Fig. 6(a), data point No. 3.] To make a comparison at room temperature, we let Θ_S increase at a rate similar to that of $\Theta_S(T)$ evaluated from JANAF's high-temperature data for CrN. Then, we get, at 298 K, $\Theta_S = [556(\pm 12)]$ K and $^0S = [19.8(\pm 0.5)]$ J/K mol of atoms. This agrees with the upper limit of $^0S = [18.85(\pm 1)]$ J/K mol of atoms recommended in the JANAF tables. Two other estimates, $^0S = 16.4$ J/K mol of atoms from Kubaschewski and Alcock⁴⁵ and $^0S = 18.0$ J/K mol of atoms from De Luca and Leitnaker,⁵⁴ are significantly lower than our value.

4. Cr_2N (*hP9*)

0S of Cr_2N (*hP9*) has not been measured. Figure 6(a), with $n_e = 5.67e/a$, gives $E_S = 4.0$ Ry, $k_S = [189(\pm 10)]$ N/m, $\Theta_S = [445(\pm 12)]$ K, and hence, $^0S = [24.6(\pm 0.6)]$ J/K mol of atoms. This compares well with $^0S = [24.69(\pm 1.4)]$ J/K mol of atoms estimated by Kubaschewski *et al.*,⁵⁵ but is larger than the upper limit of the estimate $^0S = [21.62(\pm 2.8)]$ J/K mol of atoms from the JANAF tables⁵³ and, also, larger than $^0S = 19.94$ J/K mol of atoms from DeLuca and Leitnaker.⁵⁴

5. CrO (*cF8*)

The phase diagram for the Cr-O system presented by Hansen and Anderko³⁰ includes only Cr_2O_3 (*hR10*) and Cr_3O_4 (*cI80*) as stable phases. A comparison with the

neighboring systems V-O and Mn-O raises the question of the stability of CrO (*cF8*), with $n_e = 6e/a$, in Cr-O. A linear extrapolation in Fig. 2 gives $E_S = [2.65(\pm 0.2)]$ Ry, $k_S = [137(\pm 11)]$ N/m, and $\Theta_S = [409(\pm 17)]$ K, which yields $^0S = [26.5(\pm 1)]$ J/K mol of atoms. An extrapolation in Fig. 3 yields $\Delta^0H = -160$ kJ/mol of atoms.

Experimental data on the Cr_2O_3 phase show, when compared with CrO , a more negative $\Delta^0H = [-227(\pm 1.7)]$ kJ/mol of atoms⁵³ but a larger $\Theta_S = 662$ K.²³ This suggests the possibility of a high-temperature stabilization of CrO , in analogy to the case of CrC (*cF8*). Because a thermodynamic description of the stable phases in the Cr-O system is not available, we cannot make a more detailed study of the lattice stability of “CrO.”

C. Manganese compounds

1. MnC (*cF8*)

The properties of MnC are discussed in Sec. VI B.

2. Mn_2N (*hP3*), Mn_3N_2 (hexagonal), and Mn_4N (*cP5*)

From Ω and Fig. 6(a) we estimate for Mn_2N ($n_e = 6.33e/a$), $E_S = 3$ Ry, $k_S = [137(\pm 10)]$ N/m, $\Theta_S = [372(\pm 14)]$ K, and hence, $^0S = [28.7(\pm 0.9)]$ J/K mol of atoms.

From the line in Fig. 6(b) we would get, for Mn_2N , $\Delta^0H = -18$ kJ/mol of atoms, which should be corrected for the anomalous E_{coh} of elemental Mn (cf. Sec. IV B). Comparing with the other Mn compounds in Fig. 6(b), we estimate that effect to amount to about $[13(\pm 2)]$ kJ/mol of atoms in Mn_2N . Thus, we estimate for Mn_2N that $\Delta^0H = -(18 + 13) = [-31(\pm 2)]$ kJ/mol of atoms. Miedema's formula³ gives $\Delta^0H = -50$ kJ/mol of atoms.

For Mn_3N_2 ($n_e = 6.43e/a$) we obtain $E_S = 2.90$ Ry, $k_S = [135(\pm 10)]$ N/m, $\Theta_S = [357(\pm 13)]$ K, and hence, $^0S = [29.6(\pm 0.9)]$ J/K mol of atoms.

The hexagonal nitrides Mn_2N_x ($0.8 < x < 1.06$) show antiferromagnetic transitions above room temperature⁵⁶ ($360 \text{ K} > T_N > 300 \text{ K}$).

For Mn_4N ($n_e = 6.6e/a$) we get $E_S = 2.75$ Ry, $k_S = [117(\pm 10)]$ N/m, $\Theta_S = [314(\pm 14)]$ K, and hence, $^0S = [32.7(\pm 1)]$ J/K mol of atoms. Yatsimirski *et al.*⁵⁷ estimated $^0S = 33.5$ J/K mol of atoms. Mn_4N is ferromagnetic with $T_c = 745$ K.

D. Iron compounds

1. FeC (*cF8*)

The properties of FeC are discussed in Sec. VI C.

2. Fe_5C_2 (*mC28*) and “ $\text{Fe}_{2.2}\text{C}$ ” (*mC28*)

The thermodynamic properties of the Fe_5C_2 (*mC28*) carbide (the so-called Hägg's carbide) are poorly known. Figure 5(a) with $n_e = 6.86e/a$, gives $E_S = [3.9(\pm 0.2)]$ Ry, $k_S = [190(\pm 10)]$ N/m, $\Theta_S = [431(\pm 12)]$ K, and hence, $^0S = [25.3(\pm 0.7)]$ J/K mol of atoms. Similarly,

Fig. 5(b) gives $\Delta^0 H = [5(\pm 2)]$ kJ/mol of atoms.

No information seems available for Fe_5C_2 , but for a carbide of the slightly different composition $\text{Fe}_{2.2}\text{C}$ ($n_e = 6.75e/a$) there is some information evaluated by Chipman.⁵⁸ Extrapolating his results to room temperature yields $^0S = 24.0$ J/K mol of atoms and $\Delta^0 H = 6.3$ kJ/mol of atoms, which is consistent with results for $\text{Fe}_{2.2}\text{C}$ using our method, $^0S = [25.0(\pm 0.6)]$ J/K mol of atoms and $\Delta^0 H = [4.3(\pm 2)]$ kJ/mol of atoms. Hägg's carbide is ferromagnetic, with $T_c = 520$ K.⁵⁸

3. Fe_7C_3 (oP40) and Fe_2C (hP3)

There seem to be no measurements of the thermodynamic properties of the so-called Eckstrom-Adcock carbide Fe_7C_3 (oP40), and the so-called Jack's carbide Fe_2C (hP3), often denoted $\epsilon\text{-Fe}_{2.3}\text{C}$. For Fe_7C_3 , Fig. 5(a) with $n_e = 6.8e/a$ gives $E_S = [3.8(\pm 0.2)]$ Ry, $k_S = [187(\pm 10)]$ N/m, $\Theta_S = [432(\pm 12)]$ K, and hence, $^0S = [25.3(\pm 0.6)]$ J/K mol of atoms. Figure 5(b) yields $\Delta^0 H = [4.5(\pm 2)]$ kJ/mol of atoms. Similarly, for Fe_2C with $n_e = 6.67e/a$, we get $E_S = [3.9(\pm 0.2)]$ Ry, $k_S = [189(\pm 10)]$ K, $\Theta_S = [445(\pm 12)]$ K, and hence, $^0S = [24.6(\pm 0.6)]$ J/K mol of atoms. Further, we estimate $\Delta^0 H = [3.5(\pm 2)]$ kJ/mol of atoms, to be compared with $\Delta^0 H = -2$ kJ/mol of atoms from Miedema's formula.³ Fe_7C_3 and the ϵ carbide are reported as ferromagnetic, with $T_c = 523$ K (Ref. 31) and $T_c = 643$ K (Ref. 58), respectively.

E. Cobalt compounds

1. Co_2C (oP6)

An orthorhombic (oP6) phase with the formula Co_2C has been reported in the Co-C system,³¹ but reliable information on its thermodynamic properties is lacking. Figure 5(a) with $n_e = 7.33e/a$ gives $E_S = [3.4(\pm 0.2)]$ Ry, $k_S = [167(\pm 10)]$ N/m, $\Theta_S = [411(\pm 12)]$ K, and hence, $^0S = [26.4(\pm 0.7)]$ J/K mol of atoms. Figure 5(b) gives $\Delta^0 H = [7(\pm 2)]$ kJ/mol of atoms. This is compatible with $^0S = [24.83(\pm 3.5)]$ J/K mol of atoms and $\Delta^0 H = [5.6(\pm 5.6)]$ kJ/mol of atoms, from Kubaschewski and Alcock⁴⁵ quoting results by Richardson,⁵⁹ and with $\Delta^0 H = 6$ kJ/mol of atoms from Miedema's formula.³

2. Co_2N (oP6)

Figure 6(a) gives, for Co_2N (oP6) with $n_e = 7.67e/a$ and the measured Ω , $E_S = 2.2$ Ry, $k_S = [107(\pm 10)]$ N/m, $\Theta_S = [321(\pm 15)]$ K, and hence, $^0S = [32(\pm 1)]$ J/K mol of atoms. Yatsimirski *et al.*⁵⁷ estimated $^0S = 33.5$ J/K mol of atoms. Further, from Fig. 6(b), $\Delta^0 H = [-1(\pm 2)]$ kJ/mol of atoms, while Miedema's formula³ gives $\Delta^0 H = 3$ kJ/mol of atoms.

3. Co_3N (hP8)

For Co_3N (hP8) we estimate, from Fig. 6(a) and with $n_e = 8.0e/a$, $E_S = 2.13$ Ry, $k_S = [100(\pm 10)]$ N/m,

$\Theta_S = [292(\pm 15)]$ K, and hence, $^0S = [34.4(\pm 1)]$ J/K mol of atoms. From Fig. 6(b), $\Delta^0 H = [0(\pm 2)]$ kJ/mol of atoms. The value $^0S = [24.7(\pm 1.6)]$ J/K mol of atoms, estimated by Kubaschewski and Alcock,⁴⁵ seems too low. Yatsimirski *et al.*⁵⁷ estimated $^0S = 33.5$ J/K mol of atoms. $\Delta^0 H = [2.1(\pm 4)]$ kJ/mol of atoms proposed by Hahn and Konrad⁶⁰ has a large uncertainty, while the result of Miedema's formula,³ $\Delta^0 H = 1$ kJ/mol of atoms, is consistent with our estimate.

4. Co_4N (cP5)

There seem to be no previous estimates of 0S and $\Delta^0 H$ for Co_4N . Figure 6(a) with $n_e = 8.2e/a$ gives $E_S = 2.1$ Ry, $k_S = [96(\pm 10)]$ N/m, $\Theta_S = [276(\pm 15)]$ K, and hence, $^0S = [35.7(\pm 1.4)]$ J/K mol of atoms. From Fig. 6(b), $\Delta^0 H = [0.5(\pm 2)]$ kJ/mol of atoms.

F. Nickel compounds

1. Ni_3N (hP8) and Ni_4N (cP5)

For Ni_3N (hP8), with $n_e = 8.75e/a$, we estimate from Fig. 6(a) $E_S = 2.05$ Ry, $k_S = [97(\pm 10)]$ N/m, $\Theta_S = [288(\pm 15)]$ K, and hence, $^0S = [34.7(\pm 1.3)]$ J/K mol of atoms, to be compared with the lower estimate $^0S = 30.2$ by Yatsimirski *et al.*⁵⁷ Similarly, for Ni_4N (cP5) with $n_e = 9e/a$, we get $E_S = 2.05$ Ry, $k_S = [93(\pm 10)]$ N/m, $\Theta_S = [272(\pm 15)]$ K, and hence, $^0S = [36.1(\pm 1.4)]$ J/K mol of atoms. From Fig. 6(b) we get $\Delta^0 H = [1(\pm 2)]$ kJ/mol of atoms. No previous estimates of 0S and $\Delta^0 H$ for Ni_4N seem to be available.

VIII. CONCLUSIONS

The filling of bonding or antibonding electron states gives a theoretical understanding of some correlations between the cohesive and vibrational properties, and the number of conduction electrons for some 3d transition-metal carbides, nitrides, and oxides with dominant (*p-d*) bonding. This paper exploits such ideas in depth. It has been shown that E_S , which essentially measures the bonding strength through the entropy Debye temperature Θ_S , is closely correlated to the average number of valence electrons per atom in the compound, n_e . This regularity holds not only for simple compounds of the NaCl structure, where the band structure is known, but also for carbides and nitrides of complicated structure. A similar relation is established between n_e and the enthalpy of formation $\Delta^0 H$. The correlations are so strong that our approach offers a very useful way to estimate thermodynamic properties of the considered class of compounds. As will be shown in future work, it can be generalized to cover other systems. It also points to challenging problems regarding the electron band structure in complex compounds.

We have used the present correlations to critically analyze previous values for the room-temperature entropy 0S of a large number of compounds, or generate new estimates when previous information is lacking. A similar

analysis is also made for the enthalpy of formation, $\Delta^0 H$, and we compare with the predictions of Miedema's formula.

An important feature of our method is that it can be coupled in various ways with the so-called CALPHAD approach to assessing the thermodynamics and phase diagrams of alloy systems. Our correlations provide a new way to critically analyze the experimental input of the CALPHAD optimizations, and to estimate lacking entropy data. We have also shown how our results can be used together with CALPHAD calculations to get information on the relative stability of a phase which can be stabilized by the entropy part of the Gibbs energy. This opens new

possibilities to treat the problem of phase stabilities at high temperatures.

ACKNOWLEDGMENTS

This work has been supported in part by the Swedish Natural Science Research Council. We like to thank K. A. Gschneidner, Jr. for his comments and unpublished information on the Sc-C system. The phase-diagram calculations reported here was performed at the Department of Physical Metallurgy, The Royal Institute of Technology, Stockholm.

- ¹See, e.g., work on elemental tungsten, H. J. F. Jansen and A. J. Freeman, *Phys. Rev. B* **30**, 561 (1984); H. L. Skriver, *ibid.* **31**, 1909 (1985); J. W. Davenport, M. Weinert, and R. E. Watson, *ibid.* **32**, 4876 (1985); J. W. Davenport, R. E. Watson, and M. Weinert, *ibid.* **32**, 4883 (1985); *Phys. Scr.* **32**, 425 (1985); L. F. Mattheiss and D. R. Hamann, *Phys. Rev. B* **33**, 823 (1986); C. T. Chan, D. Vanderbilt, S. G. Louie, and J. R. Chelikowsky, *ibid.* **33**, 7941 (1986).
- ²P. Zhukov, V. A. Gubanov, O. Jepsen, N. E. Christensen, and O. K. Andersen, *J. Phys. Chem. Solids* **49**, 841 (1988).
- ³F. R. de Boer, R. Boom, W. C. M. Mattens, A. R. Miedema, and A. K. Niessen, *Cohesion in Metals* (North-Holland, Amsterdam, 1989).
- ⁴O. H. Nielsen and R. M. Martin, *Phys. Rev. Lett.* **50**, 697 (1983); Y.-Y. Ye, Y. Chen, K.-M. Ho, B. N. Harmon, and P. A. Lindgård, *ibid.* **58**, 1769 (1987).
- ⁵L. Kaufman and H. Bernstein, *Computer Calculation of Phase Diagrams* (Academic, New York, 1971). See also the CALPHAD journal.
- ⁶G. Grimvall and J. Rosén, *Int. J. Thermophys.* **4**, 139 (1983).
- ⁷G. Grimvall, *High Temp.-High Pressures* **17**, 491 (1985).
- ⁸G. Grimvall and M. Thiessen, in *Science of Hard Materials*, IOP Conf. Proc. Ser. No. 75, edited by E. A. Almond, C. A. Brookes, and R. Warren (IOP, Bristol, 1986), p. 61.
- ⁹A. Fernández Guillermé and G. Grimvall, *Phys. Rev. B* **40**, 1521 (1989).
- ¹⁰J. Rosén and G. Grimvall, *Phys. Rev. B* **27**, 7199 (1983).
- ¹¹W. M. Latimer, *J. Am. Chem. Soc.* **43**, 818 (1921); **73**, 1480 (1951).
- ¹²G. Grimvall, *Int. J. Thermophys.* **4**, 363 (1983).
- ¹³L. Brewer and O. Krikorian, *J. Electrochem. Soc.* **103**, 38 (1956).
- ¹⁴A. Neckel, K. Schwarz, R. Eibler, P. Weinberger, and P. Rastl, *Berichte Bunsen Gesellschaft* **79**, 1053 (1975); A. Neckel, P. Rastl, R. Eibler, P. Weinberger, and K. Schwarz, *J. Phys. C* **9**, 579 (1976).
- ¹⁵K. Schwarz, *CRC Crit. Rev. Solid State Sci.* **13**, 211 (1987); See also K. Schwarz and A. Neckel, in Ref. 8, p. 45.
- ¹⁶H. Nowotny and A. Neckel, *J. Inst. Met.* **97**, 161 (1969); P. Weinberger, K. Schwarz, and A. Neckel, *J. Phys. Chem. Solids* **32**, 2063 (1971).
- ¹⁷D. G. Pettifor and R. Podloucky, *J. Phys. C* **19**, 315 (1986).
- ¹⁸C. D. Gelatt, A. R. Williams, and V. L. Moruzzi, *Phys. Rev. B* **27**, 2005 (1983); A. R. Williams, C. D. Gelatt, Jr., J. W. Connolly and V. L. Moruzzi, in *Alloy Phase Diagrams*, edited by L. H. Bennett, T. B. Massalski, and B. C. Giessen (North-Holland, Amsterdam, 1983), p. 17.
- ¹⁹P. Blaha, J. Redinger, and K. Schwarz, *Phys. Rev. B* **31**, 2316 (1985); V. P. Zhukov, V. A. Gubanov, O. Jepsen, N. E. Christensen, and O. K. Andersen, *Philos. Mag. B* **58**, 139 (1988).
- ²⁰D. L. Price and B. R. Cooper, *Phys. Rev. B* **39**, 4945 (1989).
- ²¹W. A. Harrison and G. K. Straub, *Phys. Rev. B* **36**, 2695 (1987).
- ²²D. Adler, in *Solid State Physics*, edited by F. Seitz, D. Turnbull, and H. Ehrenreich (Academic, New York, 1968), Vol. 21, p. 1.
- ²³A. Fernández Guillermé and G. Grimvall (unpublished).
- ²⁴E. J. D. Garba and R. L. Jacobs, *J. Phys. Chem. Solids* **50**, 101 (1989).
- ²⁵B. Jansson, Ph.D. thesis, The Royal Institute of Technology, Stockholm, 1984.
- ²⁶A. Fernández Guillermé, Ph.D. thesis, The Royal Institute of Technology, Stockholm, 1988.
- ²⁷Using the Thermo-Calc system described in, e.g., B. Sundman, B. Jansson, and J.-O. Andersson, *CALPHAD* **9**, 1 (1985).
- ²⁸G. Hägg, *Z. Phys. Chem. B* **12**, 33 (1931).
- ²⁹K. Hatsuta, *Technol. Rep. Tohoku Imperial Univ.* **10**, 680 (1932).
- ³⁰M. Hansen and K. Anderko, *Constitution of Binary Alloys* (McGraw-Hill, New York, 1958).
- ³¹S. Nagakura and S. Oketani, *Trans. Iron Steel Inst. Jpn.* **8**, 265 (1968).
- ³²H. J. Goldschmidt, *Nature (London)* **162**, 455 (1948).
- ³³J.-O. Andersson, *Int. J. Thermophys.* **6**, 411 (1985).
- ³⁴P. Gustafson, *Carbon* **24**, 169 (1985).
- ³⁵A. Fernández Guillermé and G. Grimvall, *J. Less-Common Met.* **147**, 195 (1989).
- ³⁶J.-O. Andersson, *CALPHAD* **11**, 271 (1987).
- ³⁷D. S. Bloom and N. J. Grant, *Trans. AIME* **188**, 41 (1950).
- ³⁸A. Fernández Guillermé and G. Grimvall (unpublished).
- ³⁹A. Fernández Guillermé and W. Huang, *Int. J. Thermophys.* (to be published).
- ⁴⁰W. Huang (unpublished).
- ⁴¹A. Fernández Guillermé and P. Gustafson, *High Temp.-High Pressures* **16**, 591 (1984).
- ⁴²P. Gustafson, *Scand. J. Metall.* **14**, 259 (1985).
- ⁴³H. C. Eckstrom and W. A. Adcock, *J. Am. Chem. Soc.* **72**, 1042 (1950).
- ⁴⁴F. H. Herbstein and J. A. Snyman, *Inorg. Chem.* **3**, 894 (1964).
- ⁴⁵O. Kubaschewski and C. B. Alcock, *Metallurgical Thermochemistry*, 5th ed. (Pergamon, Oxford, 1979).
- ⁴⁶S. Sato, *Sci. Papers Inst. Phys. Chem. Res. (Tokyo)* **34**, 1356 (1938), quoted in *Chem. Abstr.* **33**, 2405 (1939).

- ⁴⁷E. J. Huber, G. C. Fitzgibbon, E. L. Head, and C. E. Holley, J. Phys. Chem. **67**, 1731 (1963).
- ⁴⁸B. Neumann, C. Kröger, and H. Kunz, Z. Anorg. Allg. Chem. **218**, 379 (1934).
- ⁴⁹K. C. Mills, *Thermodynamic Data for Inorganic Sulphides, Selenides and Tellurides* (Butterworths, London, 1974).
- ⁵⁰A. Inoue and T. Masumoto, Scr. Metall. **13**, 711 (1979).
- ⁵¹J.-O. Andersson, Metall. Trans. A **19**, 627 (1988).
- ⁵²J. D. Browne, P. R. Liddell, R. Street, and T. Mills, Phys. Stat. Solidi **1**, 715 (1970); M. Nasr-Eddine and E. F. Bertaut, Solid State Commun. **9**, 717 (1971).
- ⁵³JANAF Thermochemical Tables, 3rd ed. edited by M. W. Chase, C. A. Davies, J. R. Downey, D. J. Frurip, R. A. McDonald, and A. N. Syverud [J. Phys. Chem. Ref. Data **14**, Suppl. 1 (1985)].
- ⁵⁴J. P. De Luca and J. M. Leitnaker, J. Am. Ceram. Soc. **56**, 126 (1973).
- ⁵⁵O. Kubaschewski, E. L. Evans, and C. B. Alcock, *Metallurgical Thermochemistry*, 4th ed. (Pergamon, Oxford, 1967).
- ⁵⁶M. Mekata, H. Yoshimura, and H. Takaki, J. Phys. Soc. Jpn. **33**, 62 (1972); R. Juza, Adv. Inorg. Chem. and Radiochem. **9**, 81 (1966).
- ⁵⁷V. K. Yatsimirski, M. V. Tovbin, and A. P. Markova, Teor. Eksp. Khim. **7**, 102 (1971).
- ⁵⁸J. Chipman, Metall. Trans. **3**, 55 (1972).
- ⁵⁹F. D. Richardson, J. Iron Steel Inst. **175**, 33 (1953).
- ⁶⁰H. Hahn and A. Konrad, Z. Anorg. Allg. Chem. **264**, 181 (1951).
- ⁶¹K. A. Gschneidner, Jr., in *Scandium*, edited by C. T. Horowitz (Academic, London, 1975), pp. 152–251.
- ⁶²P. V. Villars and L. D. Calvert, *Pearson's Handbook of Crystallographic Data for Intermetallic Phases* (American Society of Metals, Metals Park, OH, 1985).
- ⁶³V. Dufek, F. Petru, and V. Brozek, Monatsh. Chem. **98**, 2425 (1967).
- ⁶⁴K. A. Gschneidner, Jr. and F. W. Calderwood, *Critical Evaluation of Binary Rare Earth Phase Diagrams*, Rare Earths Information Center, Energy and Mineral Resources Research Institute (Iowa State University, Ames, 1984).
- ⁶⁵W. B. Pearson, *A Handbook of Lattice Spacings and Structures of Metals and Alloys*, (Pergamon, London, 1958 and 1967), Vols. I and II.
- ⁶⁶K. Frisk (unpublished).
- ⁶⁷A. Fernández Guillermet, Z. Metallkd. **79**, 317 (1988).
- ⁶⁸A. Gabriel, P. Gustafson, and I. Ansara, CALPHAD **11**, 203 (1987).
- ⁶⁹A. Burdese and F. Abbatista, Atti Accad. Sci. Torino, Classe Sci. Fis. Mat. Nat. **93**, 340 (1958-59). Quoted by Juza, Ref. 56.